Direct Stacking of Non-metallic Planar Porphyrin to DNA

Min-Ju Lee, Biao Jin, Hyun Mee Lee, Maeng Joon Jung,[†] Seog K. Kim, and Jong-Moon Kim[*]

Department of Chemistry, Yeungnam University, Gyeongsan, Gyeong-buk 712-749, Korea. [*]E-mail: alex830@yumail.ac.kr
[†]School of Applied Chemical Engineering, Kyungpook National University, Sangju, Gyeong-buk 742-711, Korea
Received May 22, 2008

Porphyrins generally bind DNA in two different ways with respect to the mixing ratio; monomeric binding at a low mixing ratio and outside stacking at a high mixing ratio. In the present study, CTDNA binding property of a planar structured porphyrin, 5,10,15,20-tetrakis(*N*-methyl-4-pyridin-4-yl-phenyl)porphyrin (referred to as B-TMPyP) was investigated using absorption, CD, LD, and LD[r] spectroscopies. B-TMPyP produced a bisignate CD band, even at the lowest mixing ratio, indicating that B-TMPyP may not have a monomeric binding mode. From the observations of the spectral changes to the absorption, CD, and LD spectra in mixing ratio dependent titrations, B-TMPyP seems to have a quite different stacking type compared to that for the binding of H₂TMPyP. Moreover, B-TMPyP produced a CD band of opposite shape in the Soret band region. A qualitative explanation for the observed optical differences is also given.

Key Words : DNA, Porphyrin stacking, Spectroscopy, Circular dichroism, Linear dichroism

Introduction

The binding of water soluble, cationic porphyrins have been intensively studied due to their application to the photodynamic therapy[1-3] as well as their binding affinity to synthetic and natural DNA.[4-6] The binding mode of porphyrins to DNA is diverse and depends upon the mixing ratio of porphyrin to DNA concentration, the nature of DNA, the central metal, and the peripheral substituents of the porphyrin ring. In general, the monomeric binding occurs at lower [porphyrin]/[DNA] mixing ratios, while porphyrin stacking at the outside of DNA is prevalent at higher mixing ratios.[7-9] Monomeric binding can be classified into two different types, which are affected by the porphyrin structure and nature of DNA; one being intercalation between DNA bases, with the other being external binding along the DNA groove. These binding modes are well classified by characteristic CD signals.[10,11] For natural DNA or GC-rich sequences, free-metal porphyrins or metalloporphyrins, which can sustain the planar structure, intercalate between DNA base pairs and exhibit a weak negative CD signal in the Soret absorption band. For AT sequences, porphyrins bind along the groove of DNA and exhibit a clear strong positive CD band in the same region. On the other hand, bulky peripheral substituted porphyrins and metalloporphyrins with axial ligands bind externally along the groove due to the steric problems, and exhibit a positive monomeric CD signal.[12,13] With increasing mixing ratio, the bisignate CD signal becomes apparent due to stacking at the outside of DNA, regardless of the porphyrin structure or DNA type.[10,14] This outside stacking can also be divided into two types; moderate stacking at intermediate mixing ratios and extensive stacking at high mixing ratios. These binding types are also distinguished by the characteristic CD bands in the Soret band region.

Meso-tetrakis(*N*-methylpyridinium-4-yl)porphyrin (referred to as H₂TMPyP, Figure 1a) is the most studied planar porphyrin, and produces the characteristic CD spectrum mentioned above.[15-17] According to a recent report, H₂TMPyP binds across the minor groove of AT-rich sequences in a monomeric binding manner, as found from circular and linear dichroism studies: two positively charged adjacent pyridinium rings may interact electrostatically with two negatively charged phosphate groups, which are three bases away on the opposite strands since the distance between the two positive charges on the porphyrin molecule is very similar to that between the reciprocal phosphate groups.[18] It has also been suggested that H₂TMPyP stacks at the major groove at high mixing ratio from comparisons of the circular dichroism spectra of its binding to duplex and triplex oligomeric A-T sequences.[19]

In this report, the role of the length of periphery substituents and the distance between neighboring positive charges of planar porphyrin in DNA binding property was investigated using 5,10,15,20-tetrakis(*N*-methyl-4-pyridin-4-yl-phenyl)porphyrin (referred to as B-TMPyP, Figure 1b). In the case of B-TMPyP, a benzene ring was inserted between the porphyrin ring and methylpyridiniumyl ring of H₂TMPyP, while preserving its planar structure. The comparison of spectroscopic behaviors of H₂TMPyP and B-TMPyP complexed with calf thymus DNA (refered to as CTDNA) showed that B-TMPyP may have quite a different DNA binding property.
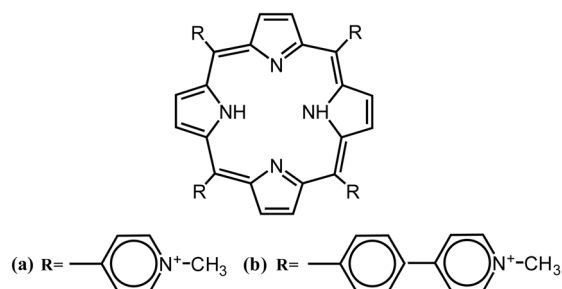
Figure 1. Molecular structure of (a) H₂TMPyP and (b) B-TMPyP.

Materials and Methods

Materials. Porphyrins were purchased from MidCentry (Chicago, IL), with all other chemicals from Sigma (Seoul, Korea) and used without further purification. B-TMPyP was dissolved in DMSO, and the molar extinction coefficient was determined spectrophotometrically. CTDNA was purchased from Worthington Biochemical Co. (Lakewood, NJ), and was dissolved in 5 mM cacodylate buffer, at pH 7.0, containing 100 mM NaCl and 1 mM EDTA (ethylenedi-aminetetraacetate) at 4 °C. The DNA solution was then dialyzed several times against 5 mM cacodylate buffer, which included 5 mM Na$^+$, at pH 7.0. This buffer was used throughout this work. The concentration was determined using the extinction coefficients: $\varepsilon_{258\,nm} = 6700$ M^{-1} cm^{-1}, $\varepsilon_{424\,nm} = 2.26 \times 10^5$ M^{-1} cm^{-1}, and $\varepsilon_{423\,nm} = 1.88 \times 10^5$ M^{-1} cm^{-1} for CTDNA, H$_2$TMPyP, and B-TMPyP, respectively, with the DNA concentration denoted as the concentration in the base.

Self-complementary [d(AT)$_n$]$_2$ oligonucleotides (where $n = 3$, and 7 corresponding to 6 and 14 AT base pairs) were purchased from Integrated DNA Technologies (Coralville, IA). The formation of the duplex was ensured by monitoring the characteristic melting curve and the fluorescence intensity of ethidium bromide. For instance, the fluorescence intensity of the [d(AT)$_3$]$_2$-ethidium mixture at 2 °C, at which all measurements were performed, was larger by a factor of ten compared to that at 40 °C. Aliquots of the concentrated porphyrins (typically ~200 μM) were added to the oligonucleotide solution to obtain the desired mixing ratios, with the spectral signals corrected for the volume changes. The concentration of DNA was fixed at 5 μM oligonucleotides. The extinction coefficient of duplex [d(AT)$_n$]$_2$ were 67000 M^{-1}cm^{-1} and 155400 M^{-1}cm^{-1} for 6 and 14mer oligonucleotides at 2 °C, respectively. The extinction coefficients were provided by the supplier's specification sheet. The mixing ratio, R, in this work is defined by the concentration ratio of [porphyrin]/[oligonucleotide] thus, $R = 1$ indicates one porphyrin molecule per 14 AT base pairs for the 14mer oligonucleotide and one porphyrin per 6 base pairs for the hexamer. Porphyrin was always added to the oligonucleotide solution last, as the mixing order can affect the binding mode of porphyrin.[20]

Spectroscopic Measurements. The absorption spectra were recorded on a Cary 100 Bio UV-Vis spectrophotometer and circular dichroism (CD) spectra on a Jasco 810 spectropolarimeter. The linear dichroism (LD) spectra were measured using a Jasco 715 spectropolarimeter equipped with a flow-orienting Couette cell device with inner-rotating cylinder, as described by Nordén and Seth.[21-23] Some of the CD and LD spectra were averaged over several scans when necessary. The measured LD was divided by the isotropic absorption to give a reduced LD (LD^r), which is related to the angle, α, which specifies the orientation of the transition moment of the drug with respect to the local helix axis of DNA:

$$LD^r = \frac{LD}{A} = \frac{A_\perp - A_\parallel}{A} = \frac{3}{2}S(3\cos^2\alpha - 1)$$

Where S is the orientation factor, such that $S = 1$ for a perfect orientation and $S = 0$ for a random orientation. The S value can be calculated by assuming an angle of 86° between the $\pi \rightarrow \pi^*$ transition of the DNA base and the DNA helix axis.[21]

Results

Absorption Spectra. The absorption spectra of H$_2$TMPyP and B-TMPyP complexed with CTDNA are depicted in Figure 2, which show similar absorption changes in the Soret band region. In the absence of CTDNA, the absorption maxima of both H$_2$TMPyP and B-TMPyP appeared at *ca* 420 nm. Upon binding to CTDNA, similar hypochromism and red-shift were shown: 45 and 41% hypochromism and 16 nm and 13 nm red-shift for H$_2$TMPyP and B-TMPyP, respectively. These may indicate that the intensities of the interactions of both porphyrins with CTDNA are quite similar.

However, they displayed distinct spectral changes in the porphyrin titrations shown in Figure 3a and 3b. The binding of H$_2$TMPyP showed a gradual decrease in absorbance at lower mixing ratios, then a small blue shift appeared, with a slight increase of absorbance for intermediate mixing ratios. This spectral change indicates that the porphyrin started to stack at the outside of the DNA stem.[10] On further increasing the mixing ratio, another blue shift and hypochromism were observed. This typical stepwise spectral change has been well defined as being due to the mixing ratio dependent change of porphyrin binding type from monomeric to moderate, as well as to extensive stacking. On the other hand, the absorbance of B-TMPyP decreased with increasing mixing ratio, without significant spectral shift in this concentration range. This indicates that B-TMPyP may have different binding characteristics with CTDNA to those of H$_2$TMPyP.

Circular Dichroism. The CD spectra of TMPyP and B-TMPyP in the presence of CTDNA are compared in Figure 4. For H$_2$TMPyP, a monomeric negative CD signal was shown in the Soret band region at the lowest mixing ratio,
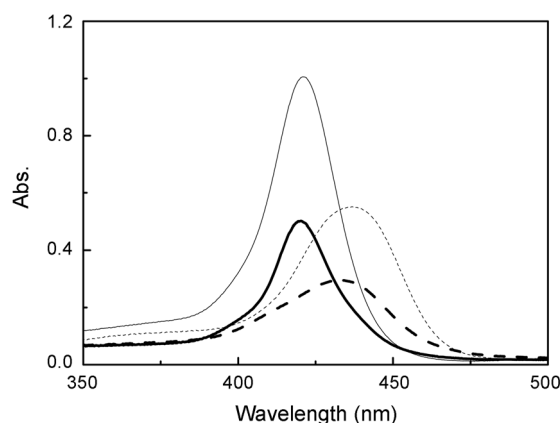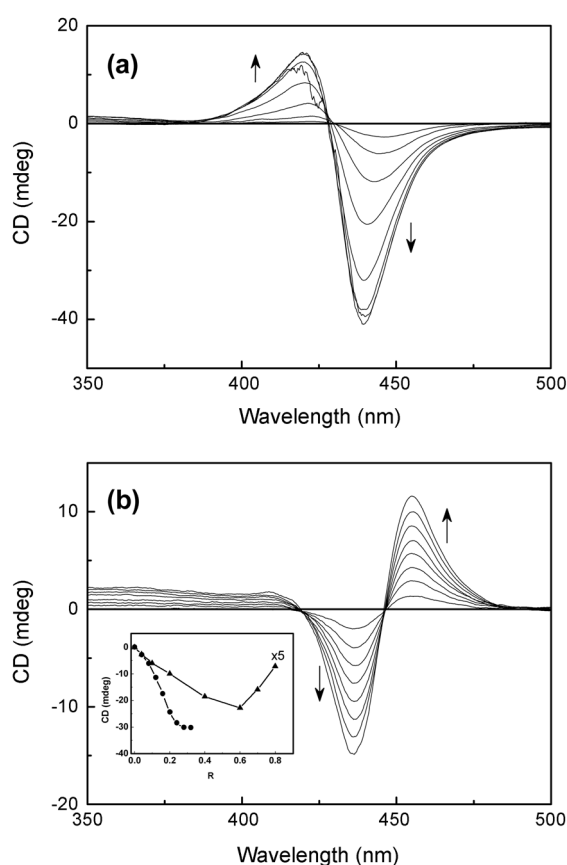

Figure 2. Absorption spectra of H$_2$TMPyP (thin lines) and B-TMPyP (bold lines) in the absence (solid line) and presence (dashed line) of CTDNA. [DNA] = 100 μM in DNA base, [porphyrin] = 4 μM.
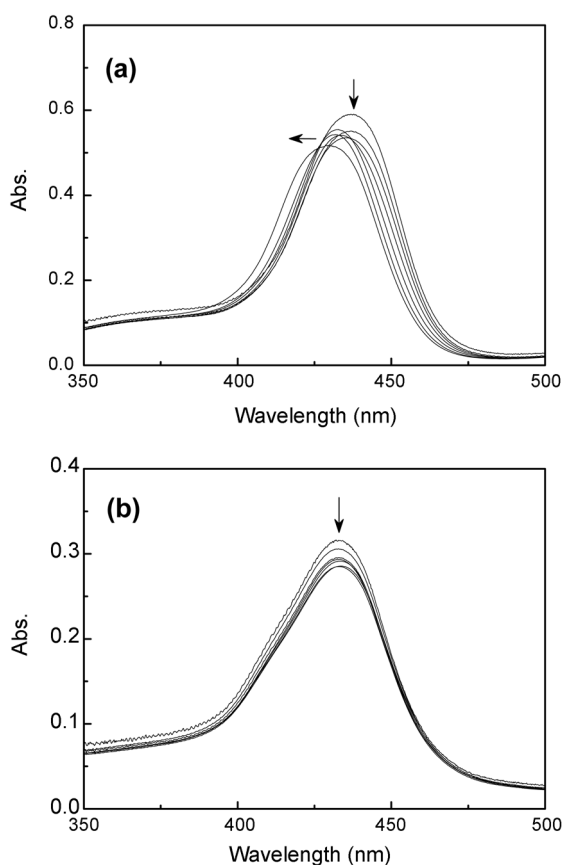
Figure 3. Absorption titration of (a) H_2TMPyP and (b) B-TMPyP to CTDNA. [CTDNA] = 100 μM. Porphyrin concentration was increased to the arrow direction according to the R ratio increase; R = 0, 0.02, 0.04, 0.08, 0.12, 0.16, 0.20 and 0.24. All spectra were normalized to 4 μM of porphyrin.

Figure 4. CD spectra of (a) H_2TMPyP and (b) B-TMPyP in the presence of CTDNA. [CTDNA] = 100 μM. Porphyrin concentration was increased to the arrow direction according to the R ratio increase; R = 0, 0.04, 0.08, 0.12, 0.16, 0.20, 0.24, 0.28, and 0.32.

R = 0.04, centered at *ca* 446 nm. This is a typical CD signal for the intercalative binding of porphyrin. On increasing the porphyrin concentration, the negative maximum started to shift to 440 nm in the shorter wavelength region, with a positive band starting to simultaneously appear around 420 nm, indicating the porphyrin molecules had started to stack at the outside of the DNA. An isochloric point at 430.5 nm for lower mixing ratios also moved to the shorter wavelength region with increasing mixing ratios. The stacking density considered to become higher with increases in the mixing ratio. The binding of B-TMPyP showed much simpler CD changes compared to those of H_2TMPyP, with a clear bisignate signal, even at the lowest mixing ratio. Moreover, the shape of the CD band, negative signal in the shorter wavelength region and positive one in the longer wavelength region, was opposite to that for the case of H_2TMPyP. With increasing the mixing ratios, the CD intensity increased proportionally to the concentration of B-TMPyP till over than R = 0.4 (Figure 4b, insert), but a plateau at R = 0.3 for H_2TMPyP. Finally over than R = 0.6, the intensity started to sharply decrease. This change appeared to be caused by the change in binding type, but the binding characteristics are remained unclear at this stage. Also, unlike the case of H_2TMPyP, the isochloric point at 446 nm did not shift on

changing the mixing ratio, indicating that B-TMPyP might have much simpler DNA binding properties or the binding mode is more conservable.

LD and Reduced LD. LD and LD^r spectra provide important information about the change of DNA conformation as well as the binding geometry of the DNA bound drug. The LD spectra of DNA-porphyrin complexes at various mixing ratios are depicted in Figures 5a and 5b. On comparing the binding of H_2TMPyP and B-TMPyP, remarkable differences were found not only in the DNA absorption region, but also in the Soret band region. H_2TMPyP binding caused apparent changes in the spectral shape of CTDNA in the 220-280 nm region, but no significant affect to the LD values up to R = 0.24. This change in the spectral shape was sustained for all mixing ratios but the LD value was almost halved at high mixing ratios; indicating that the high density of porphyrin binding can influence the orientability of DNA along the flow lines. The decrease in orientability may due to local denaturation or, more likely, bending of the DNA at the porphyrin binding site. In the Soret band region, the H_2TMPyP signal appeared at a maximum of *ca* 440 nm. On increasing the mixing ratio, the signal also increased almost proportionally to the H_2TMPyP concentration up to R = 0.24 (Figure 5b, insert), with the porphyrin signal being almost four times that of the DNA intensity. Additionally, the LD
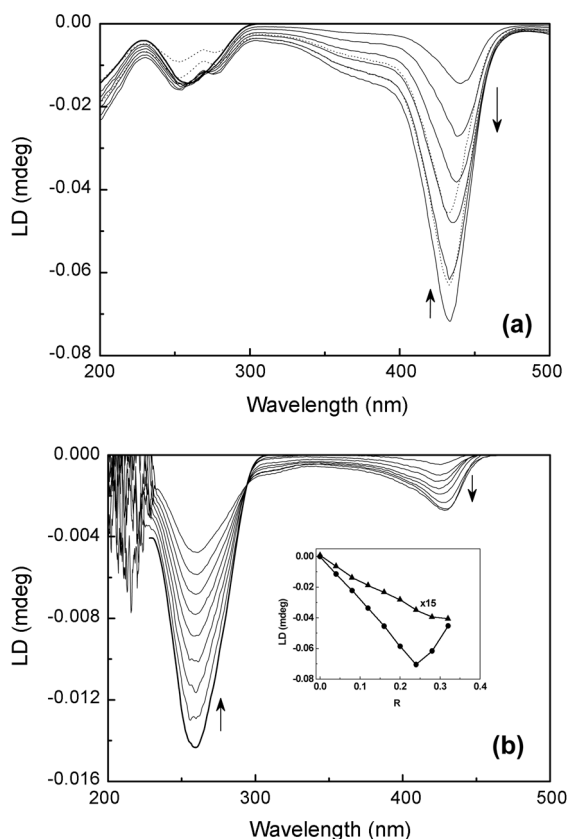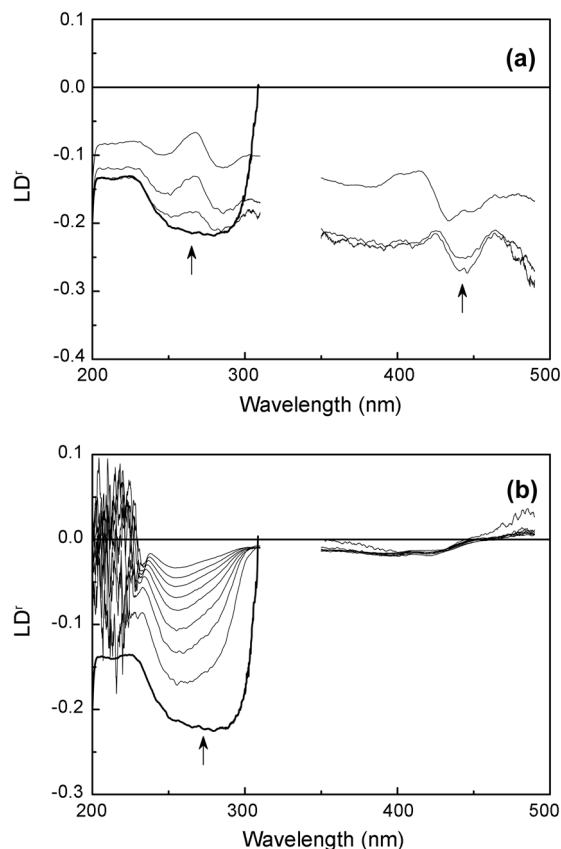
Figure 5. LD spectra of (a) H_2TMPyP and (b) B-TMPyP in the presence of CTDNA. Porphyrin concentration was increased to the arrow direction. The concentrations are the same as in Figure 3.

Figure 6. LD^r spectra (a) H_2TMPyP and (b) B-TMPyP in the absence (bold line) and presence (thin lines) of CTDNA. Porphyrin concentration was increased to the arrow direction. [DNA] = 100 μM, R = 0.04, 0.12, and 0.28.

maximum shifted to a shorter wavelength. Finally, with high mixing ratios, the LD value significantly decreased, but with no spectral shift. These drastic stepwise LD changes might be further evidence of the change in the H_2TMPyP binding mode in relation to the mixing ratio.

The binding of B-TMPyP also exhibited LD changes in both the DNA and Soret band region, while the profile of the spectral change was quite different. The LD value of DNA at 260 nm gradually decreased up to 67% on increasing the mixing ratio, but without drastic perturbation in the spectral shape, indicating consistent contribution to the orientability of DNA from B-TMPyP binding. In the Soret band region, the B-TMPyP signal appeared at a maximum of *ca* 425 nm, which gradually increased with increasing porphyrin concentration (Figure 5b, insert). Interestingly, a spectral shift to a longer wavelength; to 429 nm at R = 0.32, was also observed, which is the inverse of the case with H_2TMPyP. Moreover, the LD value was also much smaller than that of the DNA LD value. These spectral differences indicated that a different type of interaction exists for H_2TMPyP and B-TMPyP binding to CTDNA.

The LD^r spectra for the DNA complexes of H_2TMPyP and B-TMPyP are depicted in Figures 6a and 6b. Upon binding of H_2TMPyP to CTDNA, the magnitude of LD^r in the Soret band region was comparable or larger than the DNA signal in the DNA absorption region for all mixing ratios, indicat-

ing that both the x and y directions of the porphyrin system were almost parallel to the DNA bases. The porphyrin signal in the Soret band region was not constant as a function of the wavelength, which might have been due to a slight tilt of the porphyrin plane when complexed with CTDNA. With the binding of B-TMPyP, the porphyrin signals were smaller than those for the DNA. Assuming that the average angle of the DNA base pairs relative to the DNA helix axis is 86°, the average angles of the transition moment around the Soret maximum are calculated according to the equation noted in the "Materials and Methods", and they fall into the same range, $\alpha = 52 \pm 4°$. The signals were also wavelength dependent around the Soret maximum for all mixing ratios, suggesting that the porphyrin molecular plane was somewhat tilted relative to the DNA helix axis.

H_2TMPyP and B-TMPyP Binding to Oligonucleotides. In our recent report on the binding of porphyrin to various oligonucleotides,[7] the binding of H_2TMPyP was found to prefer to stack on the short double-helical DNA, while it requires a length of 8 base pairs for monomeric binding. In order to confirm the binding mode of B-TMPyP to CTDNA at low mixing ratios, the CD spectra of B-TMPyP complexed with 6 and 14 base pairs long oligonucleotides were measured, as shown in Figure 7. On binding to oligonucleotides, the CD spectra appeared to be bisignate at all the
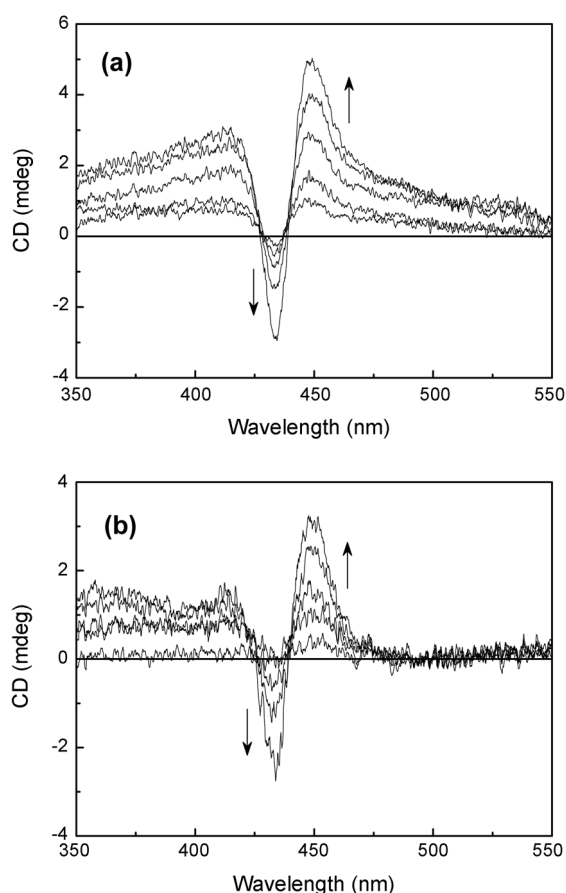
Figure 7. CD spectrum of B-TMPyP in the presence of oligomeric [(dAdT)$_3$]$_2$ and [(dAdT)$_7$]$_2$. [oligomer] = 5 μM in oligonucleotide molecule. [porphyrin] = 2, 4, 6, 8, and 10 μM. Porphyrin concentrations were increased to the arrow direction.

mixing ratios, with a negative maximum at *ca* 434 nm and a positive maximum at *ca* 448 nm for 6mer as well as for 14mer; the CD intensity also gradually increased with increasing the mixing ratio. The smallest mixing ratio, R = 0.4, corresponds to one porphyrin molecule per 2.5 oligonucleotides. In the previous work on H$_2$TMPyP binding, a monomeric CD signal started to appear from 8 base pairs long oligonucleotides, but with no monomeric CD signal for shorter lengths. This indicates that B-TMPyP may not undergo monomeric binding to CTDNA.

Discussion

In this work, the binding property of B-TMPyP to CTDNA was compared with that of H$_2$TMPyP using spectroscopic methods. As illustrated in Figure 1, B-TMPyP had longer periphery substituents and a greater distance between neighboring positive charges. The steric effect as well as positive charges of porphyrin molecules have been reported to influence the binding mode of planer porphyrin to DNA.[8,18] The possibility of the intercalative binding of B-TMPyP can be easily discarded due to its molecular size; the distance between the neighboring positive charges on the benzyl pyridinium group is about 19 Å (from the constructed model

by Hyperchem 7.0 program), which is similar to the DNA width, 19.7 Å; hence, is too big to intrude into the DNA when considering the van der Waals radii. The CD and LD data strongly support this assumption. The CD spectrum of the B-TMPyP complex showed a bisignate signal in the Soret band region, even at the low mixing ratio, but with a negative CD band for H$_2$TMPyP, which is an evidence of the intercalative binding. Moreover, a molecular angle of 52° with respective to the DNA helix axis, as obtained from the LD^r spectrum, was further evidence for the exclusion of the possibility of intercalation. Considering the distance between positive charges on the porphyrin, in addition, the minor groove of CTDNA also seems to be too narrow for B-TMPyP binding, with the binding angle of 52°, since the electrostatic interaction plays a crucial role in the porphyrin binding to DNA.[8,24,25]

An interesting phenomenon is the bisignate CD spectrum of B-TMPyP-CTDNA complex appeared in the Soret band region at the lowest mixing ratio. Similar spectral behavior was observed in the binding of TQOPP (*meso*-tetrakis[4-[(3-(trimethylammonio)propyl)-oxy]phenyl]porphine), which has long periphery substituents.[26,27] Generally, porphyrins show a monomeric CD band in the Soret band region at a low mixing ratio, regardless of their periphery substituents or the existence of a central metal; a weak negative band for intercalation or a strong positive one for external binding along the DNA groove. There are two possibilities for the unusual bisignate CD band at a low mixing ratio; one being from the abnormal binding angle of B-TMPyP to the DNA helix axis. There are two electric dipole moments laid on the porphyrin molecular plane. If both have distinctive binding angle relative to the DNA helix, they may produce inversely induced CD signals, as found in this work. The second is from the outside stacking of porphyrin without monomeric binding, even at a low mixing ratio. Porphyrins usually produce definite spectroscopic characteristics according to their DNA binding modes. The outside stacking of porphyrin can be divided into two types; moderated stacking at an intermediate mixing ratio, producing intense CD magnitude, and extensive stacking for decreased CD value compared to those for moderate stacking. This change of DNA binding mode often affects the spectroscopic behaviors, such as the absorption, CD or LD spectrum. The absorption spectrum of H$_2$TMPy, as shown in Figure 3b, is a good illustration of this change. In the low mixing ratio range, the absorption gradually decreased with increasing mixing ratio in the Soret band region. Thereafter, a small hyperchromicity was observed in the intermediate mixing ratios, which were accompanied by a small blue-shift of 4-5 nm; indicating a change in the binding mode from intercalation to moderate stacking. Lastly, a large blue-shift of about 8 nm, with a further decrease in the absorbance with the high mixing ratios indicated extensive stacking of H$_2$TMPyP. This spectral change was more extreme in the CD and LD spectra. Clear shifts of spectral maximum and isochloric point in the CD spectrum as well as an absorption-like spectral change in LD spectrum were apparent with increasing mixing ratios. All

these spectral changes were believed to be caused by the stepwise change in the binding mode from monomeric to the two different stacking modes. However, the binding of B-TMPyP does not produce comparable spectral changes in the absorption, CD, as well as LD spectra for low and intermediate mixing ratios. A distinctive spectral change was observed only with high mixing ratios, as shown in the CD spectrum (Figure 3b, insert), which may represent a change in the binding mode from moderate to extensive stacking. Further evidence is shown in the oligonucleotides binding (Figure 7). B-TMPyP produced only a bisignate CD spectrum, regardless of the DNA length. This direct stacking might also have been due to the molecular structure of B-TMPyP. Because the monomeric binding of B-TMPyP may not be allowed for the steric problem or the distance between porphyrin's positive charges, which may act as anchors in DNA binding.

The complex CD spectra in the Soret band region of H_2TMPyP and B-TMPyP raise another question, as they show opposite CD profiles; a positive band in the short wavelength region and a negative band in the long wavelength region for H_2TMPyP and vice verse for B-TMPyP. It has been already reported that this kind of CD difference is highly DNA sequence dependent.[10] In this work, however, this difference happened with the same DNA sequence. Hence, it might be derived from the different type of stacking or from the different binding site to DNA, and not from the DNA sequence. A clue for explaining this phenomenon can be drawn from the absorption spectrum shown in Figure 2. As already reported, intercalative binding displays much a larger spectral shift as well as hypochromicity in the absorption spectrum than external monomeric biding or outside stacking due to the π-π interaction between the inserted porphyrin plane and the DNA base pairs. Hence, a change from monomeric binding to outside stacking reduces both the spectral shift and hypochromicity.[28,29] Comparing the absorption change of H_2TMPyP and B-TMPyP upon binding to CTDNA, their spectral shifts as well as the hypochromicity was very similar. This similarity may suggest that the magnitude of interaction or the interaction type of B-TMPyP with CTDNA was comparable to the case of intercalated H_2TMPyP. To decide the exact binding site here would be too difficult, but it can be assumed that the molecular plane of B-TMPyP is more closely in contact with the DNA base pairs than that of H_2TMPyP for the case of outside stacking.

Conclusion

B-TMPyP probably directly stacks to the outside of CTDNA, even at the low mixing ratio due to its steric problem, even though it has planar molecular structure. In addition, the binding mode of B-TMPyP also seems to be different from that of H_2TMPyP binding to CTDNA.

References

1. Lang, K.; Mosinger, J.; Wagnerova, D. M. *Coord. Chem. Rev.* **2004**, *248*, 321.
2. Vicente, M. G. *Curr. Med. Chem. Anti-Canc. Agents* **2001**, *1*, 175.
3. Oleinick, N. L.; Evans, H. H. *Radiat. Res.* **1998**, *150*, S146.
4. Fiel, R. J. *J. Biomol. Struct. Dyn.* **1989**, *6*, 1259.
5. Marzilli, L. G. *Jew. J. Chem.* **1990**, *14*, 409.
6. Pasternack, R. F.; Gibbs, E. J. *Met. Ions. Biol. Syst.* **1996**, *33*, 367.
7. Park, T.; Kim, J. M.; Han, S. W.; Lee, D.-J.; Kim, S. K. *Biochim. Biophy. Acta* **2005**, *1726*, 287.
8. Park, T.; Shin, J. S.; Han, S. W.; Son, J. K.; Kim, S. K. *J. Phys. Chem. B* **2004**, *108*, 17106.
9. Chen, X.; Liu, M. *J. Inorg. Biochem.* **2003**, *94*, 106.
10. Lee, S.; Jeon, S. H.; Kim, B.-J.; Han, S. W.; Jang, H. G.; Kim, S. K. *Biophy. Chem.* **2001**, *92*, 35.
11. Lee, M. J.; Lee, G.-J.; Lee, D.-J.; Kim, S. K.; Kim, J.-M. *Bull. Kor. Chem. Soc.* **2005**, *26*, 1728.
12. Yun, B. H.; Jeon, S. H.; Cho, T.-S.; Yi, S. Y.; Sehlstedt, U.; Kim, S. K. *Biophys. Chem.* **1998**, *70*, 1.
13. Pasternack, R. F. *Chirality* **2003**, *15*, 329.
14. Jin, B.; Sub Shin, J.; Hwan Bae, C.; Kim, J.-M.; Kim, S. K. *Biochim. Biophy. Acta* **2006**, *1760*, 993.
15. Pasternack, R. F.; Gibbs, E. J.; Villafranca, J. J. *Biochemistry* **1983**, *22*, 5409.
16. Kruk, N. N.; Dzhagarov, B. M.; Galievsky, V. A.; Chirvony, V. S.; Turpin, P. Y. *J. Photochem. Photobiol. B* **1998**, *42*, 181.
17. Lee, Y.-A.; Lee, S.; Cho, T.-S.; Kim, C.; Han, S. W.; Kim, S. K. *J. Phys. Chem. B* **2002**, *106*, 11351.
18. Jin, B.; Lee, J.-M.; Lee, Y.-A.; Ko, J. M.; Kim, C.; Kim, S. K. *J. Am. Chem. Soc.* **2005**, *127*, 2417.
19. Lee, Y.-E.; Kim, J.-O.; Cho, T.-S.; Song, R.; Kim, S. K. *J. Am. Chem. Soc.* **2003**, *125*, 8106.
20. Ismail, M. A.; Rodger, P. M.; Rodger, A. *J. Biomol. Struct. Dyn. Convers.* **2000**, *11*, 335.
21. Matsuoka, Y.; Nordén, B. *Biopolymers* **1983**, *22*, 1713.
22. Nordén, B.; Kubista, M.; Kurucsev, T. Q. *Rev. Biophysics* **1992**, *25*, 51.
23. Nordén, B.; Seth, S. *Appl. Spectrosc.* **1985**, *39*, 647.
24. Chen, B.; Wu, S.; Li, A.; Liang, F.; Zhou, X.; Cao, X.; He, Z. *Tetrahedron* **2006**, *62*, 5487.
25. Ohyama, T.; Sasagawa, A.; Terui, N.; Mita, H.; Yamamoto, Y. *Nucleic Acids Res.* **2003**, 189.
26. Mukundan, N. E.; Pethö, G.; Dixon, D. W.; Kim, M. S.; Marzilli, L. G. *Inorg. Chem.* **1994**, *33*, 4676.
27. Mukundan, N. E.; Pethö, G.; Dixon, D. W.; Marzilli, L. G. *Inorg. Chem.* **1995**, *34*, 3677.
28. Novy, J.; Urbanova, M.; Volka, K. *Vib. Spectrosc.* **2007**, *43*, 71.
29. Wenting, A.; Xiliang, G.; Shaomin, S.; Chuan, D. *J. Photochem. Photobiol. A* **2005**, *173*, 36.